E3S Web of Conferences **569**, 05002 (2024) https://doi.org/10.1051/e3sconf/202456905002
GeoAmericas 2024

Evaluation of intermixing application of geotextiles at subgrade-base interface using accelerated pavement testing

Gino Sicha[1*], *Jorge* Zornberg[1]

[1]The University of Texas at Austin, Department of Civil Architectural and Environmental Engineering, United States of America

Abstract. This study focuses on identifying and quantifying the potential benefits of a geotextile separator in flexible pavements placed at the interface between a granular base and an underlying soft subgrade with high water content and a granular base. While benefits of using separators in roadway applications have been generally acknowledged, quantification of such benefits has been limited. The evaluation in this study is based on the results from two accelerated pavement tests using a one-third scale Model Mobile Load Simulator (MMLS3) device. Both models have identical configuration except that a non-woven geotextile was placed at the interface between the subgrade and base layer to serve as a separator in one of the pavement models. The subgrade material used in this study involved a soil mixture containing fifty percent kaolin and fifty percent Monterey sand #30. The base material was an angular AASHTO #8 aggregate. Additionally, an instrumentation program was implemented involving sensors to track the earth pressure distribution, the subgrade excess pore pressures generation, the change in moisture content of the subgrade and the horizontal particle displacement of the base layer. During exhumation of the pavement models, base and subgrade samples were collected to quantify the levels of intermixing. The results of the APT were quantified in terms of the traffic benefit ratio (TBR), which was as high as 6.4 for 25.4 mm rutting showing the significant benefit of using a non-woven geotextile as a separator to extend the design life of flexible pavements. The differences in performance observed between the control and the separation pavement models were found to correlate well with the amount of intermixing observed at the interface between subgrade and base layers. A series of soil columns were tested using cyclic loading to extend the intermixing analysis to different subgrade types with different fine content and geotextiles. The study concluded that higher levels of fine contain in the subgrade would lead to higher levels of intermixing. A correlation between the pore size of the geotextiles and the pumping of subgrade into the base was identified suggesting that smaller pore size would mitigate the pumping intermixing mechanism more efficiently.

* Corresponding author: gino.sicha@utexas.edu

1 Introduction

To understand the benefits of geotextile separators, the main pavement failure mechanisms must be studied. The principal function of a geotextile separator is to extend pavement life by reducing intermixing between base and subgrade from traffic loading [1]. Field observations have shown that geotextile separators can mitigate mechanisms that lead to intermixing [2–4]. The principal mechanisms occurring at the subgrade-base interface are: (1) intrusion of the base material into the soft subgrade due to a bearing capacity failure of base induced by traffic loading, and (2) pumping of fines form the subgrade towards the base layer due to excess pore water pressure induced by traffic/dynamic loading [1]. Even small amount of intermixing may lead to important decrease in pavement's service life [5]. [6] It has been observed that higher pumping levels of subgrade high percentage of fine particles in subgrades along with high water content and important difference in subgrade-base grain size distribution. [7] showed that a geotextile layer at the interface can potentially avoid intrusion of base material into the subgrade. [8] observed that higher frequencies of dynamic loading may be more prone to subgrade fluidization leading to more fine pumping. As for intrusion of the base into the subgrade, [8] concluded that the increase of subgrade pore water pressure due to traffic loading may reduce the subgrade strength facilitating the intrusion of base material into the subgrade. This paper discusses the impact of geotextile separators used in roadways built under soft subgrades by using accelerated pavement testing conditions. A control and a separation pavement model were built for this study following the same construction methodology and materials. Sensors to track vertical stresses distribution, moisture content, pore pressure, base particle displacement and permanent deformation were employed for a comprehensive evaluation of the pavement model's performance. Additionally, small scale soil columns were built to extent the intermixing investigation to different types of subgrades and geotextiles.

2 Methodology and Materials

This study evaluates the results of two pavement models tested using a trafficking equipment (MMLS3). The pavement models evaluated were induced with a water table of 127 mm height. The small-scale pavement models consisted of a 152.4-mm clayed subgrade layer, 127-mm gravel base layer and 25.4-mm Hot Mix Asphalt layer. The pavement models were built above ground in two modular frames with 150mm height each which facilitated the implementation of instrumentation within the soil layers. The dimensions of pavement models were 1829 mm (6') in length, 1219 mm (4') in width and 305 mm (1') in height.

A one-third scale model mobile load simulator (MMLS3) was used for the current accelerated pavement testing program. The MMLS3 device is a unidirectional vehicle load simulator with four wheels approximately one-third the diameter of a standard truck tire (300 mm diameter). The distance between tires is 1.05 m between centerlines. The tires contact pressure to 90 psi (620.5 kPa) and have a footprint area of 34 cm2. The width of the wheel is 33mm. The frequency of the passes used in these tests was two cycles per second (2 Hz) which corresponds to 7200 axles per hour. The MMLS3 equipment is 2400 mm long, 600 mm wide and 1150 mm height [9]. A profilometer designed at The University of Texas [10] was used to scan and record the pavement models' rutting with number of cycles.

Capacitance probes were installed at different elevations within the subgrade and the base to monitor the changes in moisture content during the inundation process and testing. The capacitance probes models used were Decagon 5TE, Decagon ECH2O EC-5, and TEROS 11 manufactured by Meter. Small-sized pore pressure gauges were installed in the subgrade layer of the pavement models to measure pore water pressures due to traffic loading. The model of these sensors is KPE-200KPB manufactured by Tokyo Measuring Instruments lab.

This sensor is capable of measuring pore water pressures ranging from -98.1 to 200 kPa. Two sizes of earth pressure cells were used to track the vertical stress distribution within the pavement models induced by the trafficking equipment. A smaller version of EPCs with a 50mm diameter were placed at the top of the subgrade. A bigger version of EPC (100mm diameter) was placed in the base layer. These sensors were fabricated by Tokyo Measuring Instruments Lab. Six EPC were placed at a depth of 6.3.5 mm and 152.4 mm from the pavement surface and were installed at different distances from the wheel path. Artificial soil particles attached to tell-tales were installed in the base layer at different elevations and distances form the wheel path to measure the horizontal displacements of base aggregate due to traffic loading.

The subgrade material in this study was a soil mixture containing fifty percent of kaolin and fifty percent of Monterey sand #30. A standard proctor test was conducted on the subgrade mixture as part of the characterization of the soil following ASTM D698 [11]. The maximum dry unit weight of the subgrade mixture is 17.6 kN/m^3 at an optimum gravimetric moisture content of 16%. The specific gravity of the mixture was found to be 2.663 following ASTM D792-20 [12]. The Atterberg limits of the kaolin contained in the soil mixture showed a liquid limit (LL) of 51, a plastic limit (PI) of 30, and a plastic index (PI) of 20 following ASTM D4318-17 [13]. The base material was classified as an angular AASHTO #8 aggregate obtained from a quarry in Texas. The asphalt layer of the pavement models was classified as a thin overlay mixture class A (TOM-A). This asphalt mixture contains 6.5% binder with a specific gravity of 1.4. The theoretical specific gravity of the mixture is 2.39 and the target discharge temperature is 149 Celsius. As for the properties of the geotextiles used in this study, for pavement model 2, a thin non-woven geotextile was adopted at the subgrade-base interface. This geotextile was manufactured using polypropylene fibers. The properties of this geotextile meet the required properties stated by AASHTO M288 for a class 3 non-woven geotextile separator (>50% of elongation).

3 Results and Discussion

3.1 Rutting Analysis

Rutting profiles of the control and separation pavement models were recorded at different cycles and various locations across the wheel path as presented in section 3.3.2. Figure 1 show the average pavement model surface profiles of both pavement models. In average, the control pavement model shows about 31 mm (1.22 inches) of rutting after 100 cycles. After 710 cycles, reached at the end of testing, an average rutting of 92 mm (3.6 inches) is achieved for the control pavement models. As for the separation pavement model, about 10 mm (0.39 inches) of rutting is observed after 100 cycles. After 1000 cycles, an average rutting of 35 mm (1.4 inches) is achieved. Lastly, after 1185 cycles reached by the end of testing, an average rutting of 58 mm (2.28 inches) is achieved.

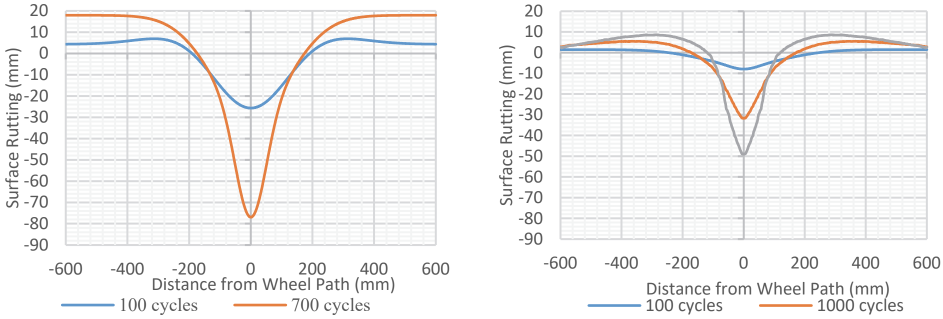

(a) (b)

Figure 1: Pavement models surface profiles at different number of cycles: (a) Control pavement model; (b) Separation pavement model.

To quantify the benefit of using geotextiles in pavements, the traffic benefit ratio (TBR) of the improved pavement model can be calculated. The TBR is defined as the ratio between the number of cycles achieved of two pavement models for a particular rutting depth. Both pavements need to have identical layer configuration and materials where the only difference should be the inclusion of a geosynthetic [14]. Since a TBR value is calculated for a particular level of rutting (failure criterion) the TBR for different levels of rutting may vary depending on the pavement layers conditions. Figure 2 shows the TBR obtained by including a geotextile separator at the different failure criteria.

The TBR increases up to 6.4 for a permanent deformation of 25.4mm showing an important improvement in pavement performance by using a geotextile separator. However, after exceeding 25 mm of surface rutting approximately, the TBR shows a considerable decrease. This behavior can be explained by the fatigue cracking failure mechanism of the asphalt layer developed at high levels of rutting. Since the TBR is an indicator of performance comparing rutting level due to surface deflection but not due to fatigue cracking, the TBR evaluation is mainly focused within the initial 25 mm of rutting.

 https://doi.org/10.1051/e3sconf/202456905002

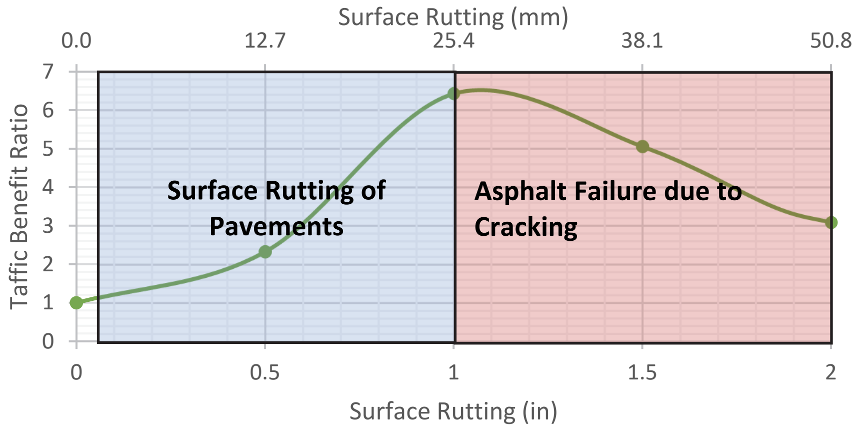

Figure 2: Traffic Benefit Ratio (TBR) for different failure criteria between separation and control pavement model.

3.2 Base Lateral Displacement

The horizontal particle displacement from the control and separation pavement models collected with the tracking array system located at different distances and depths from the wheel path showed relevant information about the lateral flow pattern of the unbound base aggregate.

Figure 3 presents contour maps of the base aggregate lateral displacements at 100, 300, and 710 cycles for the control pavement model. After 100 cycles, important levels of lateral displacement were recorded within the whole thickness closer to the wheel path (50 to 300 mm from wheel loading) of the base layer indicating a fast degradation of base modulus. This behavior could be attributed to the low stiffness of the subgrade layer resulting in a higher lateral flow of the base closer to the wheel loading. Then, after 300 cycles the lateral flow of base particles started to be more prominent on the top of the base layer closer to the wheel path reducing with distance and depth from the wheel path. At 710 cycles (end of testing) a clear pattern of lateral flow is identified. Particles have horizontally displaced though the entire thickness of the base being comparatively higher closer to the wheel path. Nevertheless, the displacements identified closer to the interface between the subgrade and base at also important, indicating a high level of base modulus degradation.

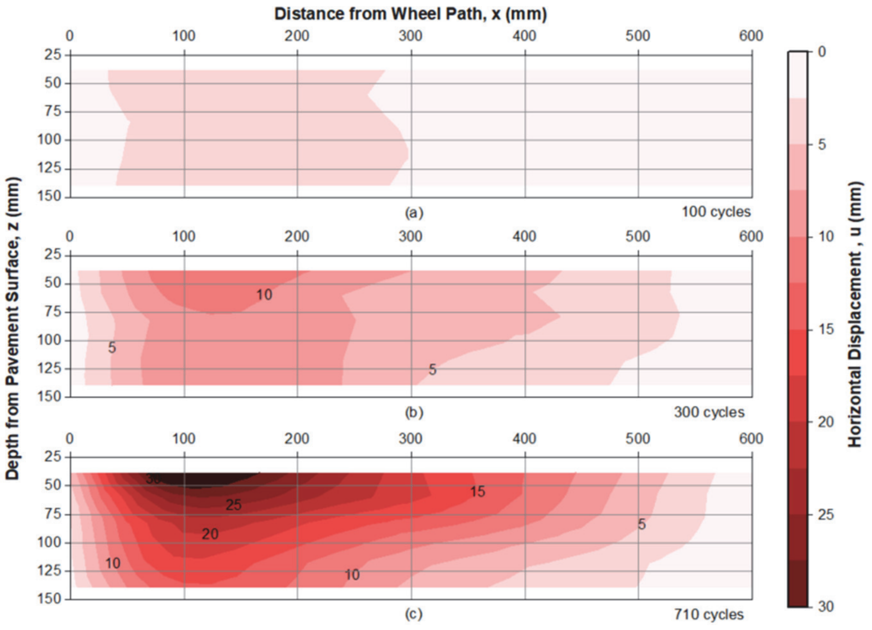

Figure 3: Contour Profile of Lateral displacement of unbound base aggregate for Control pavement model at different number of cycles: (a) 100 cycles; (b) 300 cycles; (c) 710 cycles.

The lateral displacements of the separation pavement model are presented in Figure 4 as contour maps for 100, 300, and 710, 1000 and 1180 cycles. For 100 cycles, less than 2.5mm of displacement were recorded. Nevertheless after 300 cycles, important levels of displacement are identified though the whole thickness of the base layer 50 to 250 mm from the wheel path. This behavior is not typically observed in pavements with comparatively stronger subgrade layer. Thus, the use of a soft subgrade layer may have affected the layer displacements of unbound aggregate of the base. For 710, 1000 and 1185 (end of testing) cycles a similar pattern is observed. Higher levels of displacements are identified closer to the wheel path, and they decrease with depth and distance from the wheel loading area.

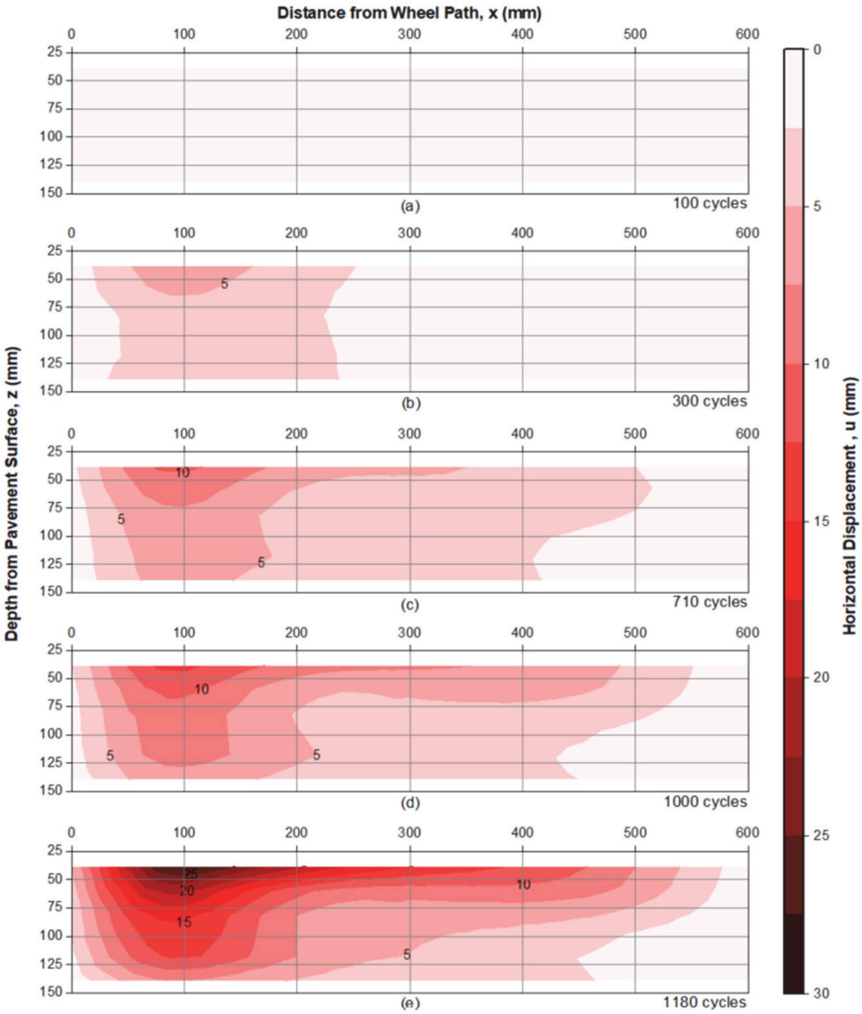

Figure 4: Contour Profile of Lateral displacement of unbound base aggregate for Separation pavement model at different number of cycles: (a) 100 cycles; (b) 300 cycles; (c) 710 cycles; (d) 1000 cycles; (e) 1180 cycles.

3.3 Pore Pressure Generation

The traffic loading exerted by the MMLS3 equipment on the pavement models with drainage intervals has a direct impact in the intermixing mechanisms occurring at the subgrade-base interface of the pavement models. Figure 5a. shows the pore pressure generation and dissipation of the control pavement models. An increase in pore pressure is observed during the loading intervals (0 to 100cycles and 100 to 710 cycles). increasing up to 2 Kpa. Between loading periods, a decrease in pore pressure is observed corresponding to the dissipation of the pore pressure. Figure 5b. shows the pore pressure data of the separation model. During cycle intervals (0-100,100-1000 and 1000-1180 cycles) an increase in pore pressure is observed up to 2 kPa approximately, After stopping the MMLS3, the pore pressure seems to dissipate showing a similar tendency to the control pavement model. Thus, the data shows that pore pressure generation tendency was not affected using the geotextile separator since it did not influence the subgrade properties. The effect of the pore pressure generation may lead to base aggregate contamination impacting its resilient modulus and the pavement performance.

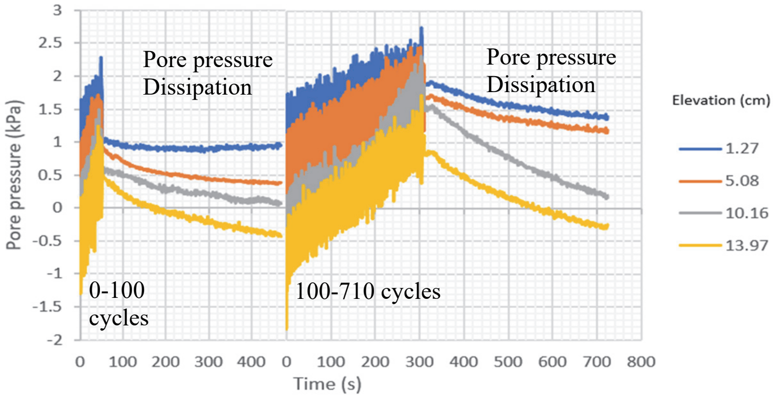

(a)

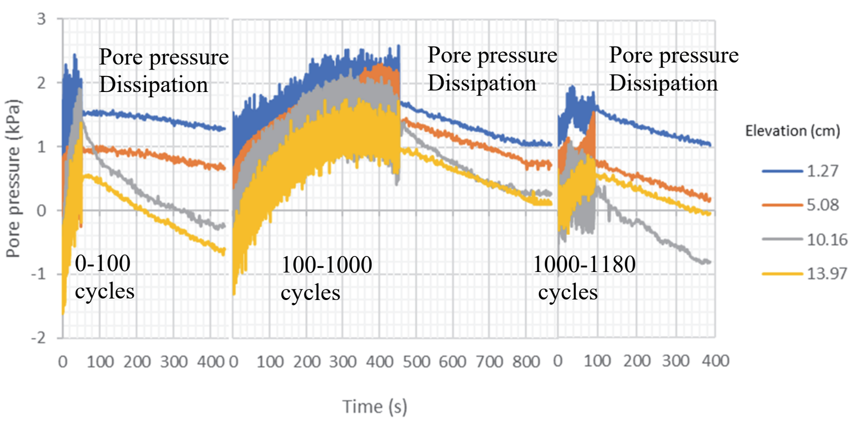

(b)

Figure 5: Pore water pressure generation and dissipation during testing process: (a) Data from control pavement model; (b) Data from separation pavement model.

3.4 Quantification of Intermixing

Samples were collected during the exhumation of the pavement model to assess an evaluation of subgrade base intermixing due to the intrusion and pumping mechanisms. The soil samples collected were 12.7 mm thick representing sub-layers of the base and subgrade to quantify the level of intermixing that occurred at failure of the pavement models. A wet sieve analysis following ASTM D5461 followed by a dry sieve analysis (ASTM D6913) was performed on the soil sample to obtain the grain size distribution. The material retained above sieve #4 was classified as “gravel” corresponding to the base material, between sieve #4 and #200 was classified as “sand” and the material passing sieve #200 was classified as “Clay”.

Figure 6 shows the percentage of the different soil types encountered in the base and subgrade sub-layers for the control and separation pavement models. The data from the control pavement model presented in Figure 6.a. shows that within 13mm below the interface, 34% of the soil weight corresponds to base material, and the rest to subgrade soil. The rest of sub-layers below the interface (below 13 mm) no gravel was encountered. Thus, the data put in evidence that for the control pavement model, the intrusion intermixing mechanism occurred within the top 13 mm of subgrade layer. Above the interface, within the first sub-layer of the base (13mm thick), 4% of sand and 4% of clay was encountered which corresponds to 8% of subgrade soil intermixed with gravel material. In the subsequent sub-layers of the base no subgrade material was encountered. The data suggest that the subgrade material was squeezed into the base because of traffic loading. The separation pavement model, Figure 6.b. shows that no intrusion of the base material into the subgrade soil occurred. Above the interface level, within the bottom 13mm of the base, 2% of clay was identified. Lower levels of pumping of fines were obtained compared to the control model. Thus, the geotextile was successfully able to provide separation of the subgrade and base layers mitigating the intermixing mechanisms induced by traffic loading.

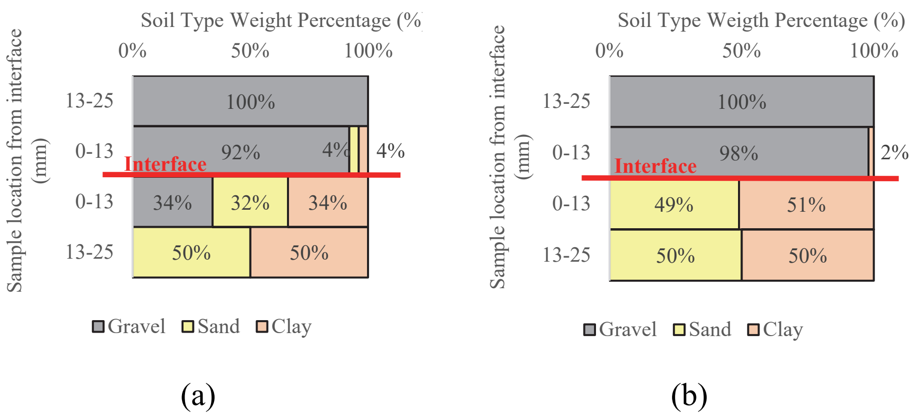

Figure 6: Intermixing profile at the interface between the subgrade and base layer of the pavement models: (a) Control pavement model; (b) Separation pavement model.

Additionally, an 'Expeditious Intermixing Test was developed to extend the intermixing analysis to different types of subgrades and geotextiles. The setup consisted of a soil column built in a modified proctor mold in which the metallic mold was replaced by a transparent acrylic mold of 305mm (12") high and 101.6mm (4") diameter. The acrylic was cut at 152.4mm (6") which corresponds to the subgrade-base interface location. A drainage geocomposite 10.16mm thick (geonet sandwiched by non-woven geotextiles) was installed at the bottom for the soil column mold to distribute water evenly during the inundation process. The subgrade material was placed in one lift of 40.6mm, one lift of 50.8mm, one lift of 38.1mm and one lift of 12.7 mm at an initial moisture content of 11.5%. The clay mixtures were compacted to a dry density of 90% of relative compaction standard proctor. For the test in which pure sand was tested as a subgrade, the soil was compacted to a unit weight of 15.8 kN/m^3 corresponding to dense sand. Then, a geotextile was placed at the top of the subgrade if required. The base granular material was placed dry (w=0%) in two lifts of 50.8mm and 25.4 mm and compacted to a unit weight of 16kN/m^3. After finishing construction, the soil columns were submerged in a container with 127mm water. The inundation process was performed for 7 days. Then, the columns were tested using a cyclic load of 600 kPa at a frequency of 2 Hz for 1,000 cycles.

The results obtained from the expeditious soil column testing program are presented in Figure 7. The plots show the weight percentage of gravel (base material), sand, and clay (subgrade materials). Below the interface elevation, the percentage of base material encountered was interpreted as the level of intermixing due to intrusion of base aggregate mechanism. The subgrade material identified above the interface line was interpreted as the level of intermixing due to the pumping of subgrade mechanism. Figure 7a. shows that the specimen with dense sand subgrade without geotextile showed minor intrusion (4%) and pumping (2%) within 13mm from the interface, indicating negligible subgrade-base contamination. Figure 7b. shows the results of a Subgrade with 20% kaolin and 80% sand without geotextile. It exhibited higher intrusion (28%) and pumping (8%) levels compared to a dense sand subgrade. Figure 7c. shows the results of a soil column with a subgrade mixture containing 50% of kaolin and 50%. In this test, 36% of intrusion was identified in the top 13 mm of the subgrade showing an increase with respect to test 1 and 2. Above the interface, within the bottom 13 mm of the base, 8% of subgrade soil was found in which 4 % corresponded to sand and 4% to clay. For the sublayers located 13 to 25mm and 25 to 38mm from the bottom base, 2% and 1% of clay were identified respectively showing a higher level of subgrade pumping compared to tests 1 and 2. Figure 7d. shows the results from a pure kaolin subgrade. The percentage of intrusion observed below the interface was 45% within the top 13 mm of subgrade. For the subgrade sublayer located between 13mm and 25mm from the interface, 10% of base material was encountered. Thus, the intrusion intermixing mechanism was comparatively higher for a pure kaolin subgrade than for subgrades containing sand such as in test 1, 2 and 3. As for subgrade pumping, 14%, 6% and 2% of fines were observed in the bottom three base sublayers corresponding to base samples collected 0-13mm,13-25mm and 25-38mm from the interface respectively. Thus, higher levels of pumping were identified when using pure kaolin as a subgrade. Figure 7e. shows the results from soil column with a subgrade soil mixture containing 50% of kaolin and 50% of sand as well as a non-woven geotextile (GT1) placed at the subgrade-base interface to provide separation of the layers. In this case, no base intrusion was observed in the subgrade. On the other hand, only 2% of fines were identified in the bottom sublayer of the subgrade. Figure 7f. shows the results from a soil column with a subgrade mixture containing 50% of kaolin and 50% of sand and a woven geotextile (GT2) was placed at the subgrade-base interface. As in test 5 (using a geotextile separator), no base intrusion was identified within the subgrade. On the other hand, 5% of subgrade material (2% of sand and 3% of kaolin) was observed in the bottom 13mm of the base. Lower levels of subgrade pumping were identified compared to the control soil column (Test 3). When comparing the results to test 5 higher pumping levels were identified which can be correlated to the pore size of the woven geotextile (GT2) which was two twice as big as the geotextile use in test 5 (GT1).

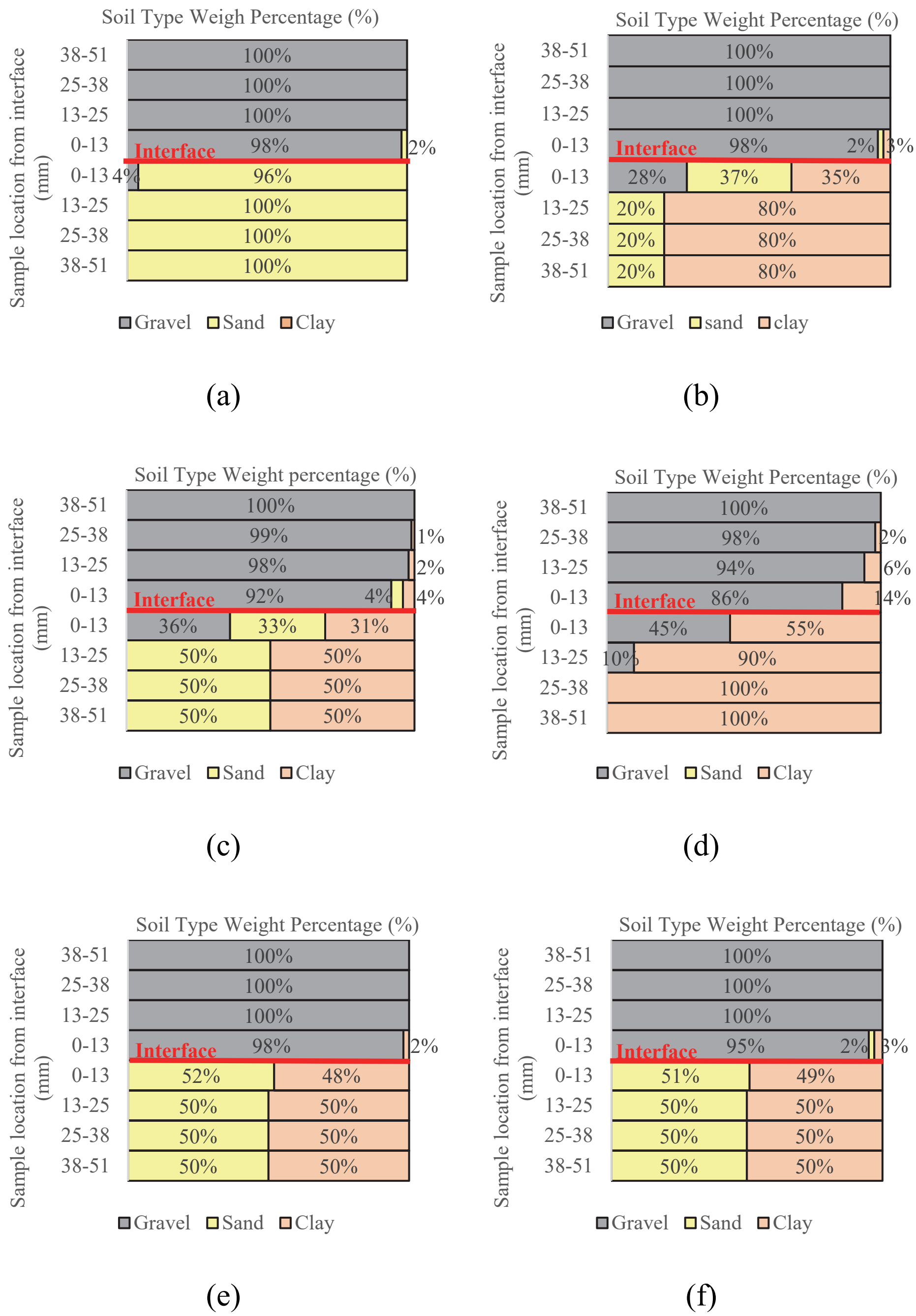

Figure 7: Test results from Expeditious Intermixing Testing for different subgrade mixtures: (a) Test 1: Pure Sand; (b) Test 2: 20% Kaolin and 80% Sand; (c) Test 3: 50% Kaolin and 50% Sand ; (d) Test 4: Pure Kaolin; (e) Test 5: 50% Kaolin and 50% Sand Subgrade and geotextile 1; (f) Test 6: 50% Kaolin and 50% Sand Subgrade and geotextile 2.

4 Conclusions

This study assessed geotextile separators at the subgrade-base interface using an Accelerated Pavement Test (APT) program. Testing focused on intermixing under high subgrade saturation, fines, and loading frequency. One model was a control without geotextile. The other used a low stiffness non-woven geotextile for separation only. Additionally, small scale tests involving soil columns and cyclic loading were performed to extent the intermixing analysis. The following conclusions were drawn from the experimental evaluation presented in this study. The geotextile greatly improved pavement performance up to 25mm rutting in the APT conditions, demonstrating potential benefits in soft subgrades. The maximum Traffic Benefit Ratio was 6.4 at 25mm rutting. The intrusion of unbound granular base particles into the subgrade soil was identified as the governing mechanism of intermixing. The level of intrusion depended on the difference in grain size distribution between the base material and subgrade soil. The finer the subgrade soil compared to the base material; the more intrusion was identified. The use of geotextiles fully mitigated the intrusion mechanism. Pumping of subgrade soil into the base layer was identified as a secondary mechanism of intermixing. The data suggests that the pumping intermixing mechanism occurred due to the vertical flow because of the pore pressure generation built during traffic loading. The higher level of fines level resulted in higher contamination of the base. The pore size of the geotextile relative to the subgrade grain size distribution was an important factor to mitigate the pumping intermixing mechanism. Smaller pore size of geotextiles minimized the filtration of subgrade soils with high fine content reducing the base contamination. The results of this investigation put in evidence the benefits of a geotextile as a separator of subgrade and base in soft subgrade with high water content. These results are particularly relevant due to the lack of field data available regarding the quantification of the benefit offered by geotextile used for separation.

The authors gratefully acknowledged the financial support provided by Solmax for this research. The authors acknowledged Kangwei Chen for his contribution in the development of the APT program.

References

1. R. M. Koerner, *Designing with Geosynthetics*, 6th ed (Xlibris Corp., Indianapolis, Ind.?, 2012).
2. A. Loulizi, I. L. Al-Qadi, S. A. Bhutta, and G. W. Flintsch, Transportation Research Record **1687**, 104 (1999).
3. I. L. Al-Qadi and A. K. Appea, Transportation Research Record **1849**, 212 (2003).
4. M. S. Hossain and Benjamin Neale Schmidt, *Benefits of Using Geotextile Between Subgrade Soil and Base Course Aggregate in Low-Volume Roads in Virginia* (Virginia Transportation Research Council, 2009).
5. J. G. Zornberg, Procedia Engineering **189**, 298 (2017).
6. I. Alobaidi and D. Hoare, Geosynthetics International **1**, 221 (1994).
7. I. Alobaidi and D. J. Hoare, Geosynthetics International **6**, 241 (1999).
8. J. Arivalagan, C. Rujikiatkamjorn, B. Indraratna, and A. Warwick, Geotextiles and Geomembranes **49**, 1324 (2021).
9. A. L. Epps, T. Ahmed, D. C. Little, and F. Hugo, *Performance Prediction with the MMLS3 at Westrack* (Texas Transportation Institute, 2001)
10. S. Sankaranarayanan, Evaluation of Mechanisms Governing the Stabilization of Unbound Aggegate Bases by Geogrids in Flexible Pavements, The University of Texas at Austin, (2023).

11. ASTM International, *D698-12 Standard Test Methods for Laboratory Compaction Characteristics of Soil Using Standard Effort (12,400 Ft-Lbf/Ft3 (600 kN-m/M3))* (2021).
12. ASTM International, (2020).
13. ASTM International, (2017).
14. AASHTO, (2009).